3D fine scale ceramic components formed by ink-jet prototyping process

R. Noguera, M. Lejeune, T. Chartier

ENSCI - SPCTS –UMR 6638, 47 à 73, Avenue Albert Thomas

87065 Limoges Cedex (FRANCE)

Abstract

Different investigations have been carried out to optimize an ink-jet printing technique, devoted to the fabrication of 3D fine scale ceramic parts, by adjustment of the fluid properties of the ceramic suspensions and by controlling the ejection and impact phenomena. A 10 vol% PZT loaded suspension characterized by a Newtonian behavior corresponding to a viscosity of 10mPa.s and to a ratio $Re/We^{1/2}$ of 5.98 has been selected. The ejection and impact phenomena strongly depend on the driving parameters of the printing head, in particular the formation of the droplet, with satellite or not, as well as its velocity and volume are function of the pulse amplitude. Moreover, the conditions of ejection (droplet velocity and volume) control the characteristics of the deposit (definition, spreading, thickness uniformity). Green PZT pillar array corresponding to the skeleton of 1-3 ceramic polymer composite for imaging probes has been achieved by ink-jet printing with a definition equal to 90µm.

Keywords: printing, suspensions, PZT, ejection, impact.

1- Introduction

Ink-jet printing process has been recently explored as a solid freeforming fabrication (SFF) technique to produce 3D ceramic parts [1-11]. Numerous solid freeform fabrication techniques to form ceramic parts have been developed during the last decade. They consist in building ceramic parts by depositing the material, layer by layer, on the basis of computer-aided design (CAD) files of the structures. By a simple modification of the file, it

becomes possible to change the configuration of the component; therefore, these methods are specifically appropriate to generate 3D complex ceramic structures without expensive tooling for prototypes or even for small productions. The prototyping techniques developed up to now for ceramic parts such as the stereolithography [12-16], the fused deposition modeling [17-18] and the selective laser sintering [19] are characterized by definition around 150µm, and don't allow to deposit different materials on the same layer. In comparison, ink-jet printing prototyping process opens the way to the development of multifunctional 3D fine scale ceramic parts.

In fact, ink-jet printing prototyping process consists in the deposition of ceramic system micro-droplets (a few pl) ejected via nozzles to build the successive layers of the 3D structures. Consequently, by adjustment of the aperture of the printing head and the control of the spreading phenomenon of the droplet, one can expect to reach a standard definition around 50µm which could finally decrease to 10µm, in taking into account the tremendous evolution in the printing field. Moreover, this technique exhibits the additional capability to deposit different materials on the same layer via a multi-nozzle system.

Consequently, thanks to its high flexibility in terms of design because of its capability to deposit different materials with a high definition, this technique may be applied in particular to the production of sophisticated microelectronic devices integrating metallic connection network (packaging, microactuators or sensors……).

The recent developments concerning the fabrication of ceramic parts by ink-jet printing techniques are carried out according two routes: (i) the deposition of hot-melted ceramic loaded wax [5-7], which solidifies by impact on cold substrate or (ii) the deposition of ceramic suspensions which dry by evaporation of the solvent that uses systems initially devoted to ink-jet printing on paper [1-4,8-11].

This paper is focused on the second route, in the case of a drop-on-demand type technique, which consists to eject an ink drop at the good place and time by actuating a piezoelectric element [20]. A specific equipment has been achieved at SPCTS laboratory with a system of printing head displacement characterized by a resolution of 0.5µm, a reproducibility of 2µm and an accuracy of 2µm. Added to an optimization of the suspension and to an adjusted electric driving of the printing heads, this equipment is very promising for the fabrication of ceramic parts with high definition i.e. corresponding to 10µm in the X/Y plane and to 1µm in the Z direction. Consequently, in order to reach these objectives, different investigations have been carried out to optimize the process through (i) the adjustment of the fluid properties of the ceramic suspensions (ii) the control of the ejection and impact phenomena.

2. Adjustment of the fluid properties of the ceramic volatile suspensions

At first, the particle size distribution of the powder must be adjusted in order that a ratio of 50 between the radius of the nozzle aperture and the $Ø_{90}$ of the powder should be obtained to avoid the blocking of the nozzle. Consequently, in our case, as the aperture of the printing head is equal to 60µm, the $Ø_{90}$ of the PZT powder is adjusted by attrition milling to 1µm.

Then, the suspension formulation was optimized in terms of the nature and of the content of the different organic compounds (solvent, dispersant, binder…) and of the ceramic loading, in order (i)to avoid sedimentation, (ii)to control the drying phenomenon : the drying rate must be high enough to minimize drop spreading but premature drying of the ink within the nozzle must be suppressed to avoid clogging, (iii)to adjust the fluid properties of the organic/ceramic suspensions in terms of viscosity and surface tension to be compatible with the type of printing head i.e. to 5-20mPa.s and 35-40 mJ/N respectively in our case and so

that the ratio $Re/We^{1/2}$ would be in the adequate range (1-10) for ejection of a consistent droplet. In fact successful drop ejection occurs when the ratio $Re/We^{1/2}$ has a value ranged between 1 and 10 with $\frac{Re}{\sqrt{We}} = \frac{\sqrt{\sigma.\rho.r}}{\eta}$, where Re is the Reynolds number ($v.r.\rho/\eta$), We is the Weber number ($v^2.r.\rho/\sigma$), ρ, η and σ are the ink density, viscosity and surface tension respectively, r the radius of the nozzle and v the fluid velocity. When this ratio is too low, viscous forces are dominant that implies large pressure for ejection; inversely, if this ratio is too high a continuous column is ejected that can lead to the formation of satellite drops behind the main drop. The figure 1 illustrates the different cases observed according to the value of $Re/We^{1/2}$ by capturing stroboscopically backlit images using a CCD camera system.

The PZT ceramic suspensions, prepared with a volume percent of binder equivalent to ceramic powder in order to guarantee a good green mechanical strength, exhibit a Newtonian behavior. Figure 2 shows the dependence of the viscosity and the ratio $Re/We^{1/2}$ with the ceramic loading. A 10 vol% ceramic loaded suspension corresponding to a viscosity of 10mPa.s and to a ratio $Re/We^{1/2}$ of 5.98 has been selected for the further investigations.

3. Control of the ejection and impact phenomena

As the definition of the ink-jet printed ceramic structures strongly depends on the velocity, the initial size and the path of the droplet just before spreading, it is essential to control these different characteristics as a function of the driving parameters of the printing head. To obtain this data, this successively requires (i)the acquisition of the ejection images via a CCD camera, (ii)the image treatment and, (iii) the analysis of the image to extract the

position of the droplet as a function of the time and consequently the corresponding instantaneous velocity as well as the droplet volume. Figure 3 shows the instantaneous velocity of the droplet and its corresponding volume as a function of the amplitude of the electric pulse. This reveals that the increase of the amplitude (up to 79V) leads to the formation of a satellite droplet [2], which catches up with the main one later [3]. Moreover, this shows that the final droplet velocity and volume increase with the amplitude of the pulse (figure 4).

Then, we have characterized the impact phenomenon as a function of the droplet velocity (figure 5). The dimensions of the dried droplet were measured thanks to a laser interferometer. At first, the minimum diameter of the dried droplet (i.e. the highest definition) corresponds to the lowest velocity. However, the spreading factor, corresponding to the ratio of the dried droplet diameter per the initial droplet diameter, is minimum for the highest droplet velocity. This can result from the variation of the evaporation mechanism and of the segregation phenomenon of the powder during impact, according to the droplet velocity.

Consequently, the topography of dried droplets has also been acquired by laser interferometer (figure 6) in order to control the morphology of the deposit. One can observe that there is a gradient of deposit thickness from the edge to the center, mainly due to the segregation of powder on the edge because of the high density of PZT (d = 7.65). However this phenomenon is less pronounced for high droplet velocity (figure 7), which leads consequently to a better thickness uniformity of the deposit in this case.

4. Fabrication of PZT parts by ink-jet printing

In order to demonstrate the feasibility of 3D fine scale ceramic parts by ink-jet printing, our investigations have been focused on the case of the PZT skeleton of 1-3

piezoelectric ceramic polymer composite used for medical imaging probes (figure 8). In fact, the ink-jet printing process could lead to the evolution of medical imaging probes in terms of performances thanks to the improvement (i) of their spatial resolution by generating fine ceramic structures (ii) and of their configuration by integration of internal electrodes by direct metal printing and more generally by variable size, shape and distribution of ceramic rods inside the probes.

The figure 9 illustrates the type of green ceramic pillar array, i.e. the ceramic skeleton of 1-3 composite, built by ink-jet printing of the ceramic suspension defined in the part 2, i.e. corresponding to a 10 vol% PZT loaded suspension. Moreover, this structure corresponds to a 50 vol% PZT loading. According to the impact results (part 3), this structure is characterized by a growth rate around 3µm/layer and by a diameter of the bottom of each pillar equal to 110µm. In comparison, the mean section of the rods is finer i.e. around 90µm. Consequently, even if some processing parameters need to be improved to optimize the characteristics of the structure, these first results are very promising: in particular, the specificities of our equipment in terms of printing head micropositionning allow to avoid the defect of mis-registration observed in previous printing trials of similar pillar arrays [11].

Apart from the fabrication of PZT pillar structures for medical probes, the ink-jet printing process is also very promising for the fabrication of other PZT devices, such as piezoelectric micromotors for in vivo drug delivery or medical diagnosis [21]. One can expect, in this case, to substitute the bulk ceramic piezoelectric element of micromotors by a multilayer structure via the direct deposition of the metallic ink thanks to a multi-nozzle system. This will lead to the reduction of the voltage down to low value (around 10V) in order to be compatible with the application as intestinal capsule.

Acknowledgement. The authors would like to express their gratitude towards the European Community (the European Social Funds) and the Limousin Region for their financial support of the present work."

References

1.P. F. Blazdell, J. R. G. Evans, M. J. Edirisinghe, P. Shaw, M. J. Binstead. The computer aided manufacture of ceramics using multilayer jet printing. *J. Mat. Sci. Lett.* 1995, **14**, 1562 - 1565.

2. M. Mott, J.H. S, J. R. G. Evans. Microengeneering of ceramics by direct ink-jet printing. *J. Am. Ceram. Soc.* 1999, **82** – 7, 1653-1658.

3.M. Mott and J. R. Evans. Zirconia/alumina functionally graded material made by ceramic ink-jet printing. *Mat. Sci. and Eng*. 1999, **A271**, 344 - 352.

4.Q. F. Xiang, J. R. G. Evans, M. J. Edirisinghe and P. F. Blazdell. Solid freeforming of ceramics using a drop-on-demand jet printer. *Proc Instn Mech Engrs* 1997, **211** part B, 211 - 214.

5.N. Reis, K. A. M. Seerden, B. Derby, J. W. Halloran and J. R. G. Evans. Direct ink-jet deposition of ceramic green bodies I – II. *Mat. Res. Soc. Symp. Proc.* 1999,. **542**, 141 - 151.

6.N. Reis, K. A. M. Seerden, B. Derby, J. W. Halloran and J. R. G. Evans and P. S. Grant. Ink-jet printing of wax-based alumina suspension. *J. Am. Ceram. Soc*. 2001, **84**, 2514-2520.

7.N. Reis, B. Derby, C. Ainsley. Freeform fabrication by controlled droplet deposition of powder filled melts. *J. Mat. Sci.* 2002, **37**, 3155-3161.

8. A. R. Bhatti, M. Mott, J. R; G. Evans, M. J. Edirisinghe. PZT pillars for 1-3 composites prepared by ink-jet printing. *J. Mat. Sci. Lett*. 2001, **20**, 1245 - 1248.

9. M. M. Mohebi, J. R. G. Evans. A drop-on-demand ink-jet printer for combinatorial libraries and functionally graded ceramics. *J. Comb. Chem*. 2002, **4**, 267-274.

10. W. D. Teng and M. J. Edirisinghe. Development of continuous direct ink jet printing of ceramics. *British Ceramic Transactions* 1998, **97**-4, 169-173

11. X. Zhao, J. R. G. Evans, M. J. Edirisinghe and J. H. Song. Ink-jet printing of ceramic pillar arrays. *J. Mat. Sci*. 2002, **37**, 1987-1992

12. Bertsch. Microstéréolithographie par masquage dynamique. Thèse de doctorat. Institut National Polytechnique de Lorraine, France, 1996.

13. C. Hinczewski, S. Corbel and T. Chartier. Ceramic suspensions suitable for stereolithography. *J. Eur. Ceram. Soc.* 1998, **18**, 583

14. F. Doreau, C. Chaput and T. Chartier. Stereolithography for manufacturing ceramic parts. *Advanced Engineering Materials*. 2000, **2** (8), 493

15. C. Hinczewski, S. Corbel and T. Chartier. Stereolithography for the fabrication of ceramic three-dimensional parts. *Rapid Prototyping J.* 1998, *4 (3)*, 104.

16. T. Chartier, C. Chaput, F. Doreau and M. Loiseau. Stereolithography of structural complex ceramic parts. *J. Mat. Sc.* 2002, **37**, 3141-3147.

17. Song et al. Development of metal-polymer composites for fused deposition modelling. *Proceedings of the 7th European Conference of Rapid Prototyping and manufacturing, Nottingham,* 1998

18. Lous et al. Fabrication of piezoelectric ceramic/polymer composite transducers using fused deposition of ceramics. *J. Am. Ceram. Soc*. 2000, . **83** – 1, 124 - 128.

19. Tolochko et al. Fabrication of micromechanical component by laser sintering of fine powders. *10th European Conference on Rapid Prototyping and Manufacturing*, Paris, 2001.

20. S. I. Zoltan. Pulsed droplet ejecting system. U.S. Patent. 3,683,212, 1970

21. D. Guyomar, TH. Mazoyer, J. D. Sauzade, M. Gschwind, C. EL Hassani, T. Mitsuta. High torque rotating motor. *2nd Japan-France Congress on Mechatronics*, Takamatsu, 1994, 43-46.

Figure captions

Figure 1 Ejection images of suspensions showing the effect of the ratio $Re/We^{1/2}$

Figure 2 Variation of the viscosity and of the ratio $Re/We^{1/2}$ with the PZT volume percent.

Figure 3 Variation of the droplet velocity and volume as a function of the distance between the nozzle and the end of the droplet for a pulse amplitude of 65V or 79V.

Figure 4 Dependence of the final velocity and droplet volume on the pulse amplitude

Figure 5 Dependence of the dried droplet diameter and of the spreading factor on the droplet velocity

Figure 6 Topography of a dried droplet acquired by laser interferometer

Figure 7 Profiles of dried droplets according to the conditions of deposition

Figure 8 1-3 piezoelectric ceramic/polymer composite

Figure 9 Scanning electronic image of a green ceramic pillar array, corresponding to the ceramic skeleton of 1-3 composite, produced by ink-jet printing of a volatile suspension

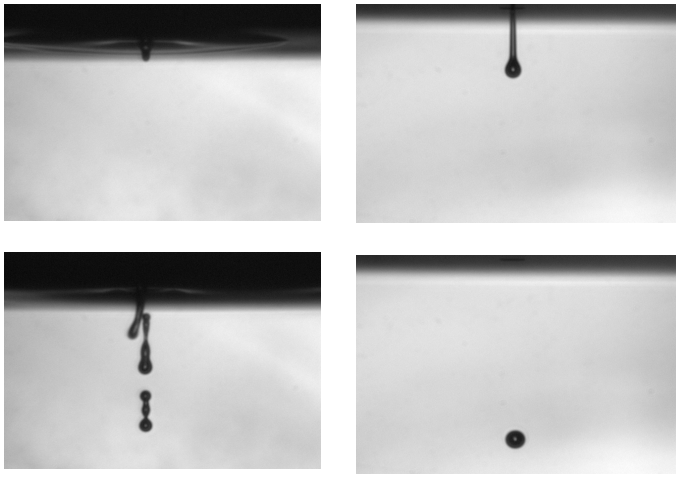

Figure 1

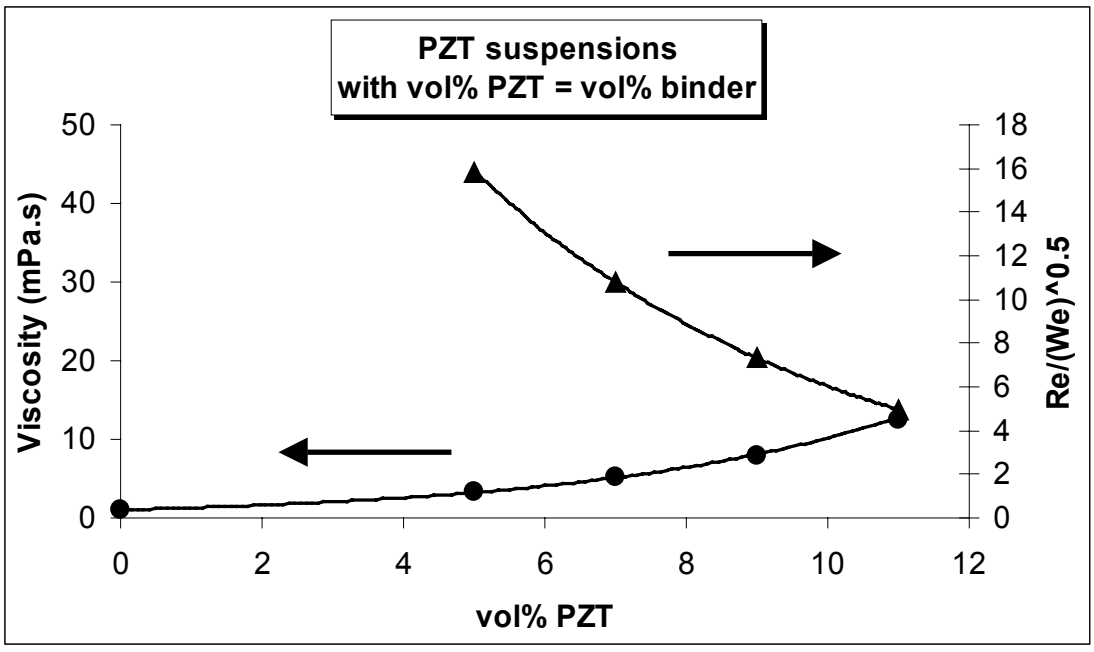

Figure 2

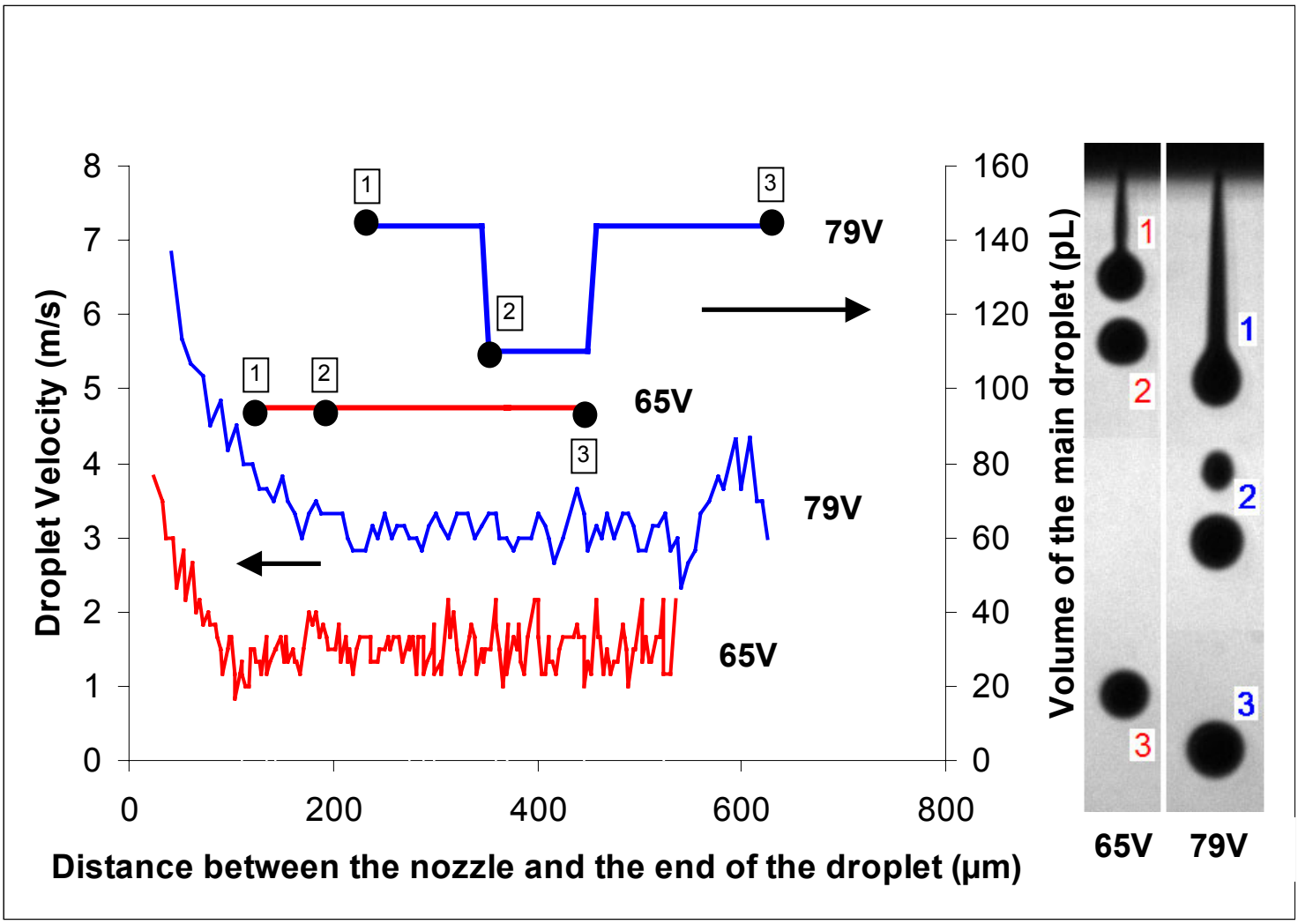
Droplet Velocity (m/s)
Volume of the main droplet (pL)
Distance between the nozzle and the end of the droplet (µm)
79V
65V
79V
65V
65V
79V
0
200
400
600
800
0
1
2
3
4
5
6
7
8
0
20
40
60
80
100
120
140
160

Figure 3

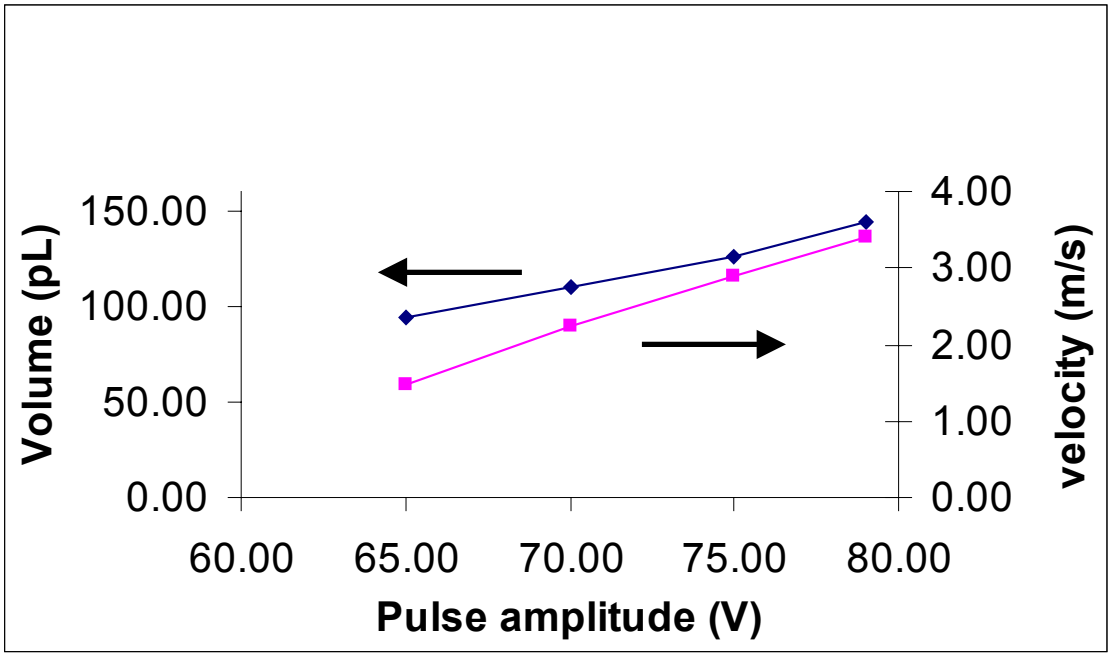

Figure 4

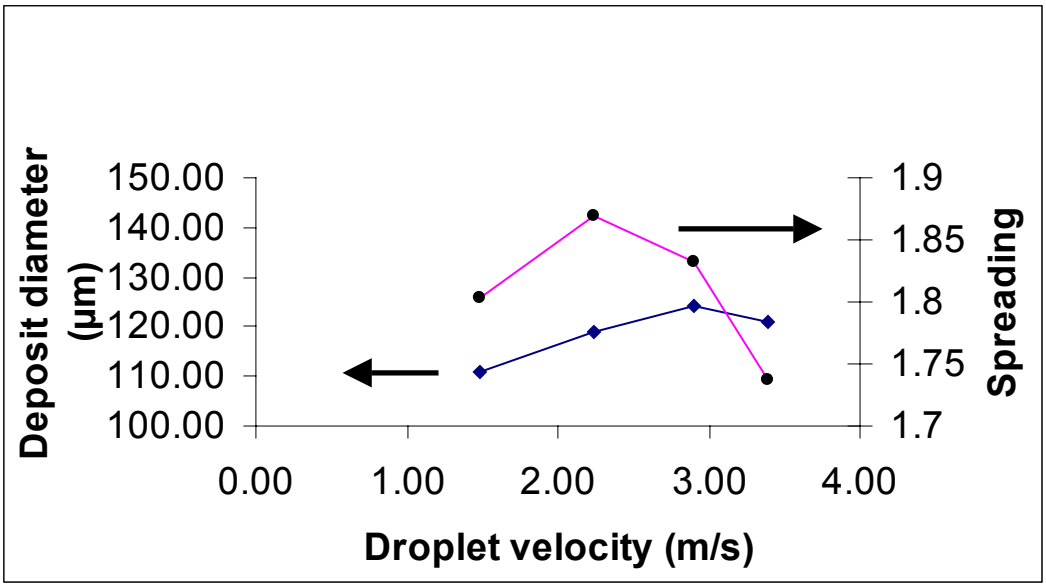

Figure 5

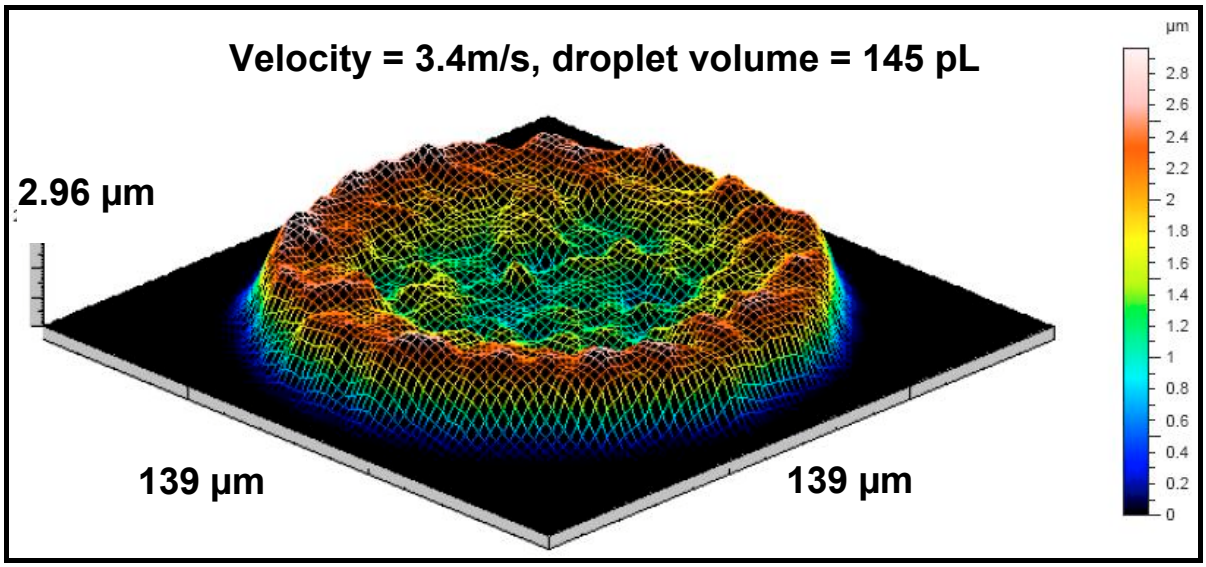

Figure 6

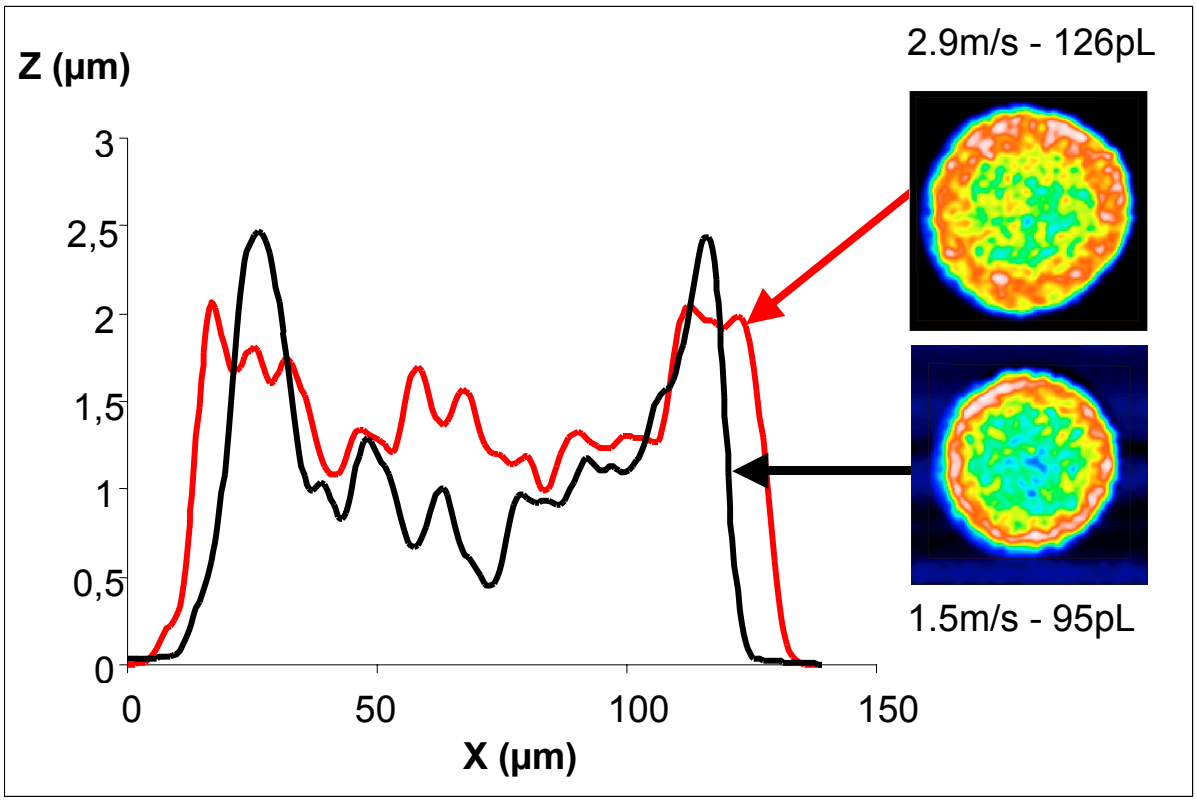

Figure 7

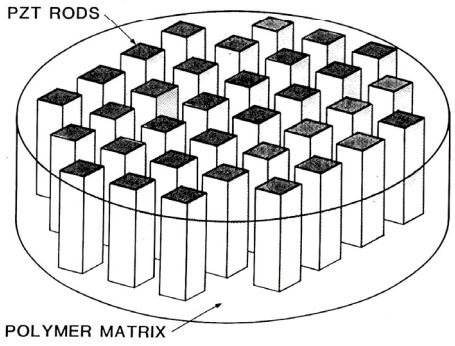

Figure 8

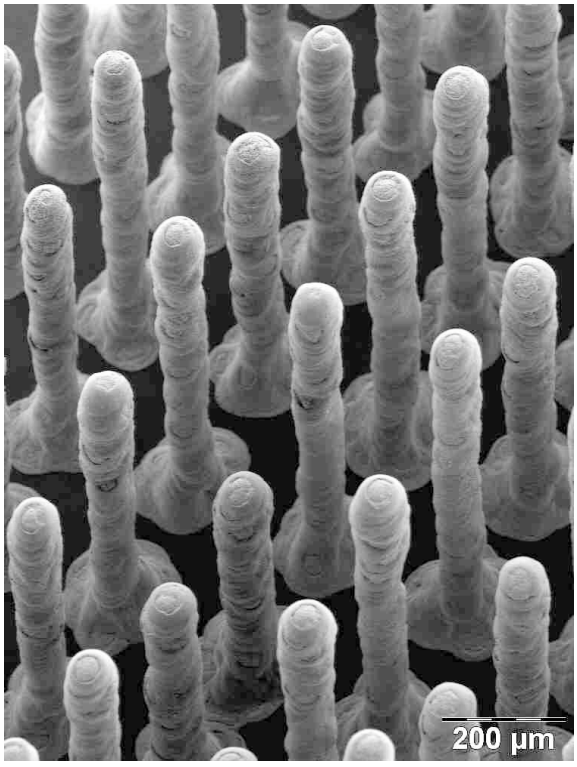

Figure 9